

# Nonaqueous liquid pool dissolution in three-dimensional heterogeneous subsurface formations

W.M.J. Bao · E.T. Vogler · C.V. Chrysikopoulos

**Abstract** A three-dimensional numerical flow and contaminant transport model is developed to investigate the effect of variable hydraulic conductivity on average mass transfer coefficients associated with the dissolution of dense nonaqueous phase liquid (DNAPL) pools in heterogeneous, water-saturated subsurface formations. Randomly generated, three-dimensional hydraulic conductivity fields are used to represent a heterogeneous confined aquifer. Model simulations indicate that the average mass transfer coefficient is inversely proportional to the variance of the log-transformed hydraulic conductivity. A power law correlation relating the Sherwood number to the variance of the log-transformed hydraulic conductivity and appropriate Peclet numbers is developed. A reasonable fit between predicted and numerically determined mass transfer coefficients is observed.

**Keywords** DNAPL pool dissolution · Heterogeneous aquifers · Variable hydraulic conductivity · Mass transfer correlations · Three-dimensional transport

## Introduction

Groundwater contamination by dense nonaqueous phase liquids (DNAPLs) is a wide-spread global concern because DNAPLs frequently enter the subsurface environment from leaking underground storage tanks, leaking pipelines, or accidental chemical spills. In the subsurface, a DNAPL migrates towards the bottom of the aquifer until it reaches a low-permeability layer such as bedrock where a

DNAPL pool may form and eventually dissolve into the groundwater (Chrysikopoulos 1995a; Khachikian and Harmon 2000).

Numerous experimental and theoretical investigations focusing on DNAPL pool dissolution in homogeneous aquifers are presented in the literature (Anderson and others 1992; Johnson and Pankow 1992; Chrysikopoulos and others 1994; Lee and Chrysikopoulos 1995; Holman and Javandel 1996; Mason and Kueper 1996; Chrysikopoulos and Lee 1998; Seagren and others 1999; Leij and van Genchten 2000; Sciortino and others 2000; Tatalovich and others 2000; and Chrysikopoulos and others 2002, to mention a few). However, aquifer properties that may affect groundwater flow and transport are known to be highly spatially variable (Chrysikopoulos 1995b). The variability of subsurface formation properties traditionally is characterized stochastically (Christakos 1992), and has been shown to influence DNAPL pool formation (Freeze 1975; Sudicky 1986) as well as pool dissolution (Rivett and others 1994; Vogler and Chrysikopoulos 2001). Furthermore, empirical correlations for the rate of interface mass transfer at single component NAPL pools have been developed for various pool geometries (Kim and Chrysikopoulos 1999; Chrysikopoulos and Kim 2000; Chrysikopoulos and others 2000; Dela Barre and others 2002). These correlations are applicable to water-saturated, homogeneous formations, and do not account for spatially variable hydraulic conductivity.

The work presented here examines the dissolution of a DNAPL pool in a heterogeneous, confined aquifer. Appropriate overall mass transfer coefficients are determined numerically for various stochastically generated hydraulic conductivity fields and groundwater velocities. Furthermore, a mass transfer correlation is developed that accounts for the variance of the log-transformed hydraulic conductivity.

## Model development

### Physical model

The physical model considered is illustrated in Fig. 1 and represents a three-dimensional, heterogeneous, confined aquifer with length  $L=7.9$  m, width  $W=8.3$  m, and height  $H=1.1$  m. A rectangular, single-component DNAPL pool is at the bottom of the aquifer. The rectangular pool has dimensions  $l_x=2.0$  m along the flow direction and  $l_y=1.6$  m

Received: 25 June 2002 / Accepted: 23 September 2002

Published online: 20 November 2002

© Springer-Verlag 2002

W.M.J. Bao (✉) · E.T. Vogler · C.V. Chrysikopoulos  
Department of Civil and Environmental Engineering,  
University of California, Irvine, CA 92697, USA  
E-mail: costas@eng.uci.edu  
Tel.: +1-949-8248661  
Fax: +1-949-8243672

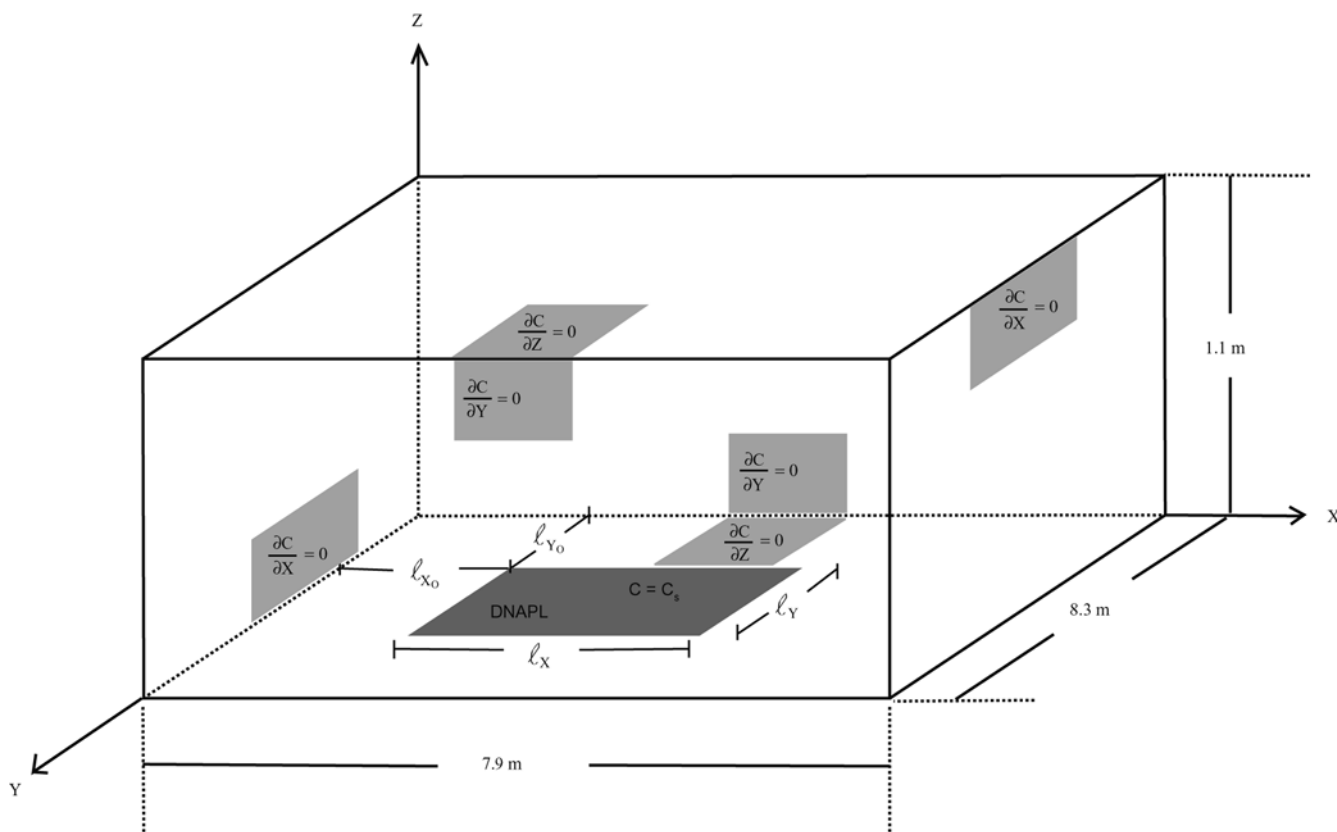


**Fig. 1**  
Schematic illustration of the aquifer domain considered in this study, showing the DNAPL pool location and the boundary conditions

lateral to the flow direction. The origin of the rectangular pool is at  $l_{x_0}=3.5$  m and  $l_{y_0}=3.0$  m. Steady groundwater flow is maintained by constant head boundaries at the influent and effluent sides of the physical model. All other boundaries are considered to be no-flux boundaries. It is assumed that the NAPL phase is immobile, and the porous medium is fully saturated with water and the hydraulic conductivity is time invariant. Furthermore, the aquifer porosity is assumed constant, because the variability in porosity is insignificant when compared to the variability in hydraulic conductivity (Freeze 1975; Dagan 1989).

### Contaminant transport

The transport of a sorbing, but nondecaying contaminant originating from a dissolving single component DNAPL pool in three-dimensional, heterogeneous, water-saturated porous media is described by the following partial differential equation:

$$R \frac{\partial C(x,y,z,t)}{\partial t} = \frac{\partial}{\partial x} \left[ D_x(x,y,z) \frac{\partial C(x,y,z,t)}{\partial x} \right] + \frac{\partial}{\partial y} \left[ D_y(x,y,z) \frac{\partial C(x,y,z,t)}{\partial y} \right] + \frac{\partial}{\partial z} \left[ D_z(x,y,z) \frac{\partial C(x,y,z,t)}{\partial z} \right] - \frac{\partial}{\partial x} [U_x(x,y,z)C(x,y,z,t)] - \frac{\partial}{\partial y} [U_y(x,y,z)C(x,y,z,t)] - \frac{\partial}{\partial z} [U_z(x,y,z)C(x,y,z,t)], \quad (1)$$

where  $x, y, z$  are the spatial coordinates in the longitudinal, lateral, and vertical directions, respectively;  $t$  is time;

$C(x,y,z)$  is the liquid phase contaminant concentration;  $D_x, D_y, D_z$  are the longitudinal, lateral, and vertical hydrodynamic dispersion coefficients, respectively;  $U_x, U_y, U_z$  are the longitudinal, lateral, and vertical interstitial fluid velocities, respectively; and  $R$  is the retardation factor described by:

$$R = 1 + \frac{\rho_b}{\theta} K_d, \quad (2)$$

where  $\rho_b$  is the bulk density of the solid matrix;  $K_d$  is the contaminant partition coefficient between the solid matrix and the aqueous phase; and  $\theta$  is the effective porosity of the aquifer.

As a DNAPL pool dissolves into the interstitial water of an aquifer, a concentration boundary layer forms over the pool-water interface. Assuming that the DNAPL pool thickness is negligible compared to the aquifer thickness, the mass transfer from the DNAPL pool into the aqueous interstitial fluid within the aquifer is described by the following relationship (Chrysikopoulos 1995a):

$$-\mathcal{D}_e \frac{\partial C(x,y,0,t)}{\partial z} = k(x,y,t)[C_s - C(x,y,\infty,t)], \quad (3)$$

where  $\mathcal{D}_e = \mathcal{D}/\tau^*$  is the effective molecular diffusion coefficient ( $\mathcal{D}$  is the molecular diffusion coefficient and  $\tau^* \geq 1$  is the tortuosity of the porous medium);  $k(x,y,t)$  is the local mass transfer coefficient;  $C_s$  is the aqueous saturation concentration of the contaminant; and  $C(x,y,\infty,t) = C_b$  is the background aqueous phase contaminant concentration. Conventionally, any location above the concentration boundary layer is considered as  $z \rightarrow \infty$ . It should be noted

that in this study the aqueous phase background concentration of the contaminant is assumed to be zero ( $C_b=0$ ). The left hand side of Eq. (3) represents Fick's law which describes the diffusive mass flux into the concentration boundary layer at the DNAPL-groundwater interface. The right-hand side of Eq. (3) represents the advective mass transfer flux.

The appropriate initial and boundary conditions for the physical system considered here are:

$$C(x, y, z, 0) = 0, \quad (4)$$

$$\frac{\partial C(0, y, z, t)}{\partial x} = \frac{\partial C(L, y, z, t)}{\partial x} = 0, \quad (5)$$

$$\frac{\partial C(x, 0, z, t)}{\partial y} = \frac{\partial C(x, W, z, t)}{\partial y} = 0, \quad (6)$$

$$\frac{\partial C(x, y, H, t)}{\partial z} = 0, \quad (7)$$

$$C(x, y, 0, t) = C_s \quad (x, y \in \mathcal{R}), \quad (8a)$$

$$\frac{\partial C(x, y, 0, t)}{\partial z} = 0 \quad (x, y \notin \mathcal{R}), \quad (8b)$$

where  $\mathcal{R}$  is the domain defined by the rectangular DNAPL-water interfacial area ( $l_{x_0} \leq x \leq l_{x_0} + l_x$ ,  $l_{y_0} \leq y \leq l_{y_0} + l_y$ ). Condition (4) indicates that there is no initial background contaminant concentration within the three-dimensional aquifer. Boundary conditions (5), (6), and (7) represent nondispersive flux boundaries. Boundary condition (8a) implies that the aqueous contaminant concentration is constant over the pool and that the DNAPL is in equilibrium with the water at the pool-water interface. Boundary condition (8b) represents a nondispersive flux boundary beyond the pool-water interface at  $z=0$ .

#### Stochastic generation of a hydraulic conductivity field

The three-dimensional aquifer considered in this study ( $L \times W \times H = 7.9 \times 8.3 \times 1.1$  m) is partitioned into  $n_x \times n_y \times n_z = 39 \times 25 \times 27$  discrete parallelepiped unit elements, where  $n_x$ ,  $n_y$ , and  $n_z$  are the number of elements along the  $x$ -,  $y$ -, and  $z$ -directions, respectively. Each  $0.2041 \times 0.3333 \times 0.0417$  m parallelepiped unit element is assigned a distinct hydraulic conductivity, as generated stochastically by the computer program SF3D (Gutjhar 1999). The hydraulic conductivity field is log-normally distributed according to the anisotropic three-dimensional exponential covariance function (Gelhar and Axness 1983; Sudicky 1986; Russo and others 1994; Lee and Chrysikopoulos 1998):

$$C_Y(\mathbf{r}) = \sigma_Y^2 \exp \left[ - \left( \frac{r_x^2}{\zeta_x^2} + \frac{r_y^2}{\zeta_y^2} + \frac{r_z^2}{\zeta_z^2} \right)^{1/2} \right], \quad (9)$$

where  $\mathbf{r} = (r_x, r_y, r_z)^T$  is a three-dimensional vector whose magnitude is the separation distance of two hydraulic conductivity measurements;  $\zeta_x$ ,  $\zeta_y$ , and  $\zeta_z$  are the correlation length scales in the longitudinal, lateral, and vertical directions, respectively; and  $\sigma_Y^2$  is the variance of the log-transformed hydraulic conductivity. A single realization of a three-dimensional, isotropic hydraulic conductivity field is shown in Fig. 2.

#### Groundwater flow

The governing three-dimensional, partial differential equation describing the steady-state groundwater flow in a heterogeneous aquifer is described by:

$$\frac{\partial}{\partial x} \left[ K(x, y, z) \frac{\partial h(x, y, z)}{\partial x} \right] + \frac{\partial}{\partial y} \left[ K(x, y, z) \frac{\partial h(x, y, z)}{\partial y} \right] + \frac{\partial}{\partial z} \left[ K(x, y, z) \frac{\partial h(x, y, z)}{\partial z} \right] = 0, \quad (10)$$

where  $K(x, y, z)$  is the spatially variable local hydraulic conductivity, and  $h$  is the piezometric (hydraulic) head. The preceding equation is a stochastic partial differential equation, because one of its parameters, namely, the local hydraulic conductivity  $K(x, y, z)$ , is a stochastic variable. The appropriate boundary conditions for flow in the physical system considered here are:

$$h(0, y, z) = h_0, \quad (11)$$

$$h(L, y, z) = h_L, \quad (12)$$

$$\frac{\partial h(x, 0, z)}{\partial y} = 0 \quad (13)$$

$$\frac{\partial h(x, W, z)}{\partial y} = 0, \quad (14)$$

$$\frac{\partial h(x, y, 0)}{\partial z} = 0, \quad (15)$$

$$\frac{\partial h(x, y, H)}{\partial z} = 0, \quad (16)$$

where  $h_0$  and  $h_L$  are the influent or upstream ( $x=0$ ) and effluent or downstream ( $x=L$ ) piezometric heads, respectively. Boundary conditions (11) and (12) represent constant piezometric heads that maintain a steady state flow through the aquifer. Boundary conditions (13), (14), (15), and (16) represent nondispersive flux boundaries.

#### Model parameters

The fluid interstitial velocities required by the contaminant transport model are evaluated by Darcy's law:

$$U_x(x, y, z) = - \frac{K(x, y, z)}{\theta} \frac{\partial h(x, y, z)}{\partial x}, \quad (17)$$

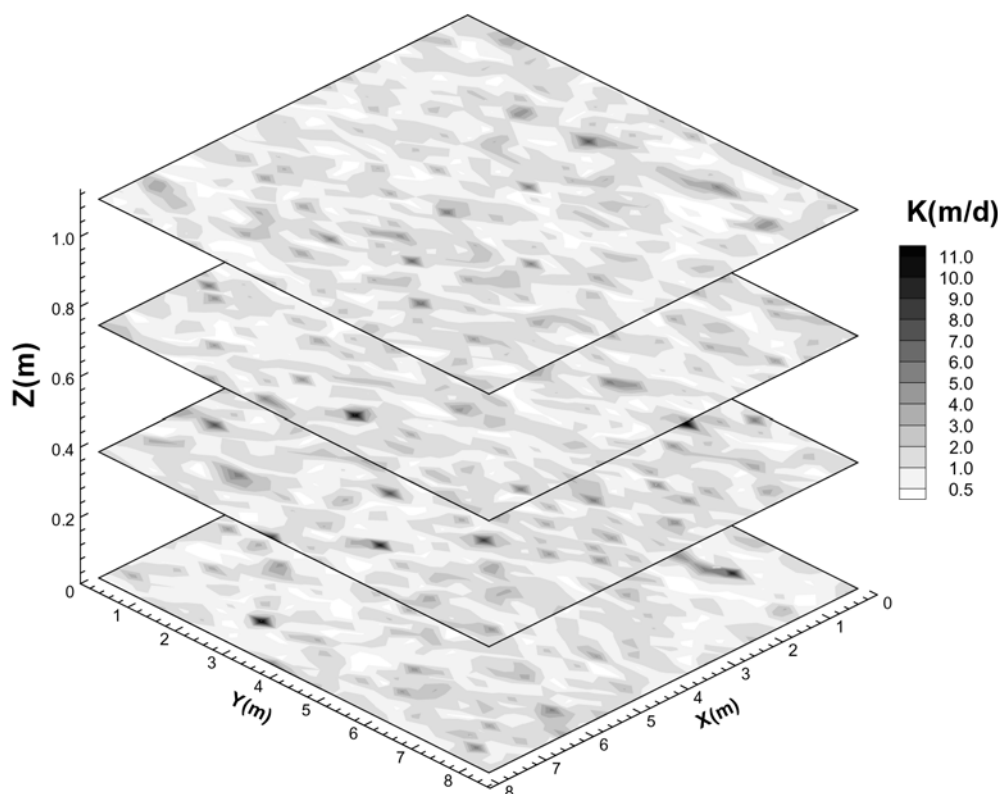


**Fig. 2**

An illustration of a three-dimensional realization of the hydraulic conductivity field. The gray scale represents the magnitude of the hydraulic conductivity (here,  $\zeta_x = \zeta_y = \zeta_z = 0.5$  m,  $\sigma_Y^2 = 0.4$ ,  $\bar{K} = 1.038$  m/h)

$$U_y(x, y, z) = -\frac{K(x, y, z)}{\theta} \frac{\partial h(x, y, z)}{\partial y}, \quad (18)$$

$$U_z(x, y, z) = -\frac{K(x, y, z)}{\theta} \frac{\partial h(x, y, z)}{\partial z}, \quad (19)$$

where  $h(x, y, z)$  is obtained from the solution to the previously described groundwater flow problem. The hydrodynamic dispersion coefficients are determined by the following equations (Bear 1979):

$$D_x(x, y, z) = \frac{\alpha_L U_x^2(x, y, z) + \alpha_T U_y^2(x, y, z) + \alpha_T U_z^2(x, y, z)}{\left[ U_x^2(x, y, z) + U_y^2(x, y, z) + U_z^2(x, y, z) \right]^{1/2}} + \mathcal{D}_e, \quad (20)$$

$$D_y(x, y, z) = \frac{\alpha_T U_x^2(x, y, z) + \alpha_L U_y^2(x, y, z) + \alpha_T U_z^2(x, y, z)}{\left[ U_x^2(x, y, z) + U_y^2(x, y, z) + U_z^2(x, y, z) \right]^{1/2}} + \mathcal{D}_e, \quad (21)$$

$$D_z(x, y, z) = \frac{\alpha_T U_x^2(x, y, z) + \alpha_T U_y^2(x, y, z) + \alpha_L U_z^2(x, y, z)}{\left[ U_x^2(x, y, z) + U_y^2(x, y, z) + U_z^2(x, y, z) \right]^{1/2}} + \mathcal{D}_e, \quad (22)$$

where  $\alpha_T$  is the transverse dispersivity, and  $\alpha_L$  is the longitudinal dispersivity.

The time-dependent average mass transfer coefficient is described by the following equation:

$$\bar{k}(t) = \frac{1}{l_x l_y N} \sum_{i=1}^N \int_{l_{x_0}}^{l_{x_0} + l_x} \int_{l_{y_0}}^{l_{y_0} + l_y} k_i(x, y, z) dx dy, \quad (23)$$

where  $N$  is the total number of log-normally distributed hydraulic conductivity field realizations considered in this study. For steady-state physicochemical and hydrodynamic conditions, it is reasonable to assume that the time-dependent average mass transfer coefficient is equal to the corresponding time-invariant average mass transfer coefficient,  $k^* = \bar{k}(t)$  (Chrysikopoulos and others 2000). Assuming that the single-component DNAPL pool consists of 1,1,2-TCA, the necessary parameter values for the simulations presented in this study are listed in Table 1.

## Numerical procedures

The piezometric head distribution throughout the model aquifer is determined by solving numerically Eq. (10) subject to the constant head boundaries given by Eqs. (11) and (12), and the no-flux boundaries given by Eqs. (13), (14), (15), and (16). A centered, finite difference approximation is employed. The spatially variable interstitial groundwater velocities are also evaluated numerically using the previously determined  $h(x, y, z)$  distribution and a centered, finite difference approximation for Eqs. (17), (18), and (19).

The governing solute transport Eq. (1) subject to initial and boundary conditions (4), (5), (6), (7), and (8) is solved

**Table 1**

Parameter values for numerical simulations

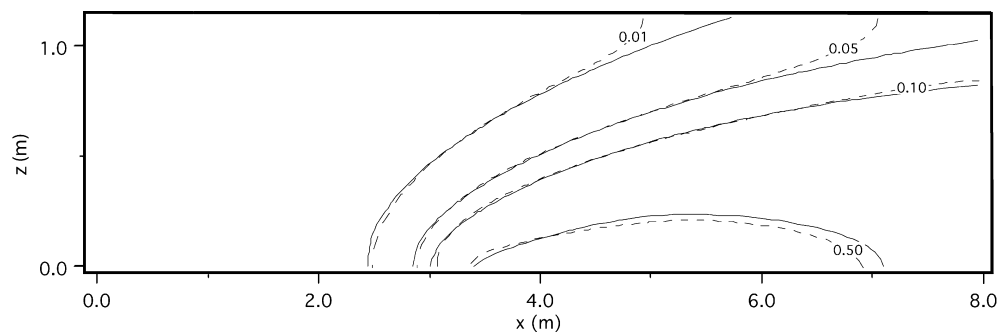
Parameter	Parameter value	Reference
$C_b$	0.0 g/l	
$C_s$	4.5 g/l <sup>a</sup>	Mackay and others (1992)
$\mathcal{D}_e$	$2.3 \times 10^{-6}$ m/h <sup>a</sup>	Chrysikopoulos and Lee (1998)
$H$	1.1 m	
$\bar{K}$	1.038 m/h	Bear (1979)
$l_x$	1.6 m	
$l_{x_0}$	3.5 m	
$l_y$	2.0 m	
$l_{y_0}$	3.0 m	
$L$	7.9 m	
$R$	1.1	Lee and Chrysikopoulos (1995)
$W$	8.3 m	
$\alpha_L$	0.3 m	Kim and Chrysikopoulos (1999)
$\alpha_T$	0.03 m	Kim and Chrysikopoulos (1999)
$\Delta t$	3 h	
$\Delta x$	0.2041 m	
$\Delta y$	0.3333 m	
$\Delta z$	0.0417 m	
$\zeta_x$	0.50 m	
$\zeta_y$	0.50 m	
$\zeta_z$	0.50 m	
$\theta$	0.3	
$\sigma_Y^2$	0.1–0.4	

<sup>a</sup>Data for 1,1,2-TCA

using the backwards-in-time alternating direction implicit (ADI) finite difference scheme. The ADI method involves solution sweeps. Concentration is solved along columns implicitly, followed by an explicit solution along the rows. Each solution sweep provides aqueous phase concentrations over one-third of the time step. A time step of  $\Delta t=3$  h was used in all simulations. The ADI method leads to a system of equations forming a tridiagonal matrix that can be efficiently solved using the Thomas algorithm (Press and others 1992). For all simulations presented here, node spacings used for the hydraulic conductivity field realizations as well as for the flow and transport modeling are held constant at  $\Delta x=0.2041$  m,  $\Delta y=0.3333$  m, and  $\Delta z=0.0417$  m.

## Comparison with analytical solution

The three-dimensional finite difference solution to the contaminant transport problem developed here is

**Fig. 3**

Comparison of dissolved concentration contours originating from a rectangular 1,1,2-TCA pool as predicted by the analytical solution (solid curves) and the numerical approximation (dashed curves) (here,  $t=3,000$  h,  $U_x=0.004$  m/h,  $U_y=U_z=0$  m/h,  $C_s=4.5$  g/l,  $l_{x_0}=3.5$  m,  $l_x=1.6$  m,  $l_{y_0}=3.0$  m, and  $l_y=2.0$  m)

compared to the three-dimensional analytical solution for rectangular NAPL pools derived by Chrysikopoulos (1995a), which, for the case of a nondecaying solute, is given by:

$$C(t, x, y, z) = \frac{C_s k^*}{4\mathcal{D}_e} \int_0^t \left( \frac{D_z}{R\pi\tau} \right)^{1/2} \exp \left[ -\frac{Rz^2}{4D_z\tau} \right] \times [\operatorname{erf}(\kappa_1) - \operatorname{erf}(\kappa_2)] [\operatorname{erf}(\zeta_1) - \operatorname{erf}(\zeta_2)] d\tau, \quad (24)$$

$$\kappa_1 = \left[ x - l_{x_0} - \left( \frac{U_x\tau}{R} \right) \right] \left( \frac{R}{4D_x\tau} \right)^{1/2}, \quad (25)$$

$$\kappa_2 = \left[ x - l_{x_0} - l_x - \left( \frac{U_x\tau}{R} \right) \right] \left( \frac{R}{4D_x\tau} \right)^{1/2}, \quad (26)$$

$$\zeta_1 = (y - l_{y_0}) \left( \frac{R}{4D_y\tau} \right)^{1/2}, \quad (27)$$

$$\zeta_2 = (y - l_{y_0} - l_y) \left( \frac{R}{4D_y\tau} \right)^{1/2}, \quad (28)$$

where  $\tau$  is the dummy integration variable. Under the special condition of a uniform interstitial fluid velocity in the longitudinal direction, the numerical and analytical solutions are compared at  $t=3,000$  h and the results are presented in Fig. 3. A reasonably good fit is observed between the numerical and analytical solution, suggesting that the numerical scheme applied in the present work is relatively accurate.

## Model simulations

Numerical simulations were performed to determine and quantify the relationship between the variance of the log-transformed hydraulic conductivity field,  $\sigma_Y^2$ , and the mass transfer coefficient associated with the dissolution of the DNAPL pool in the three-dimensional, water-saturated porous medium. For the model simulations presented here, the correlation lengths of the log-transformed hydraulic conductivity were set to  $\zeta_x=\zeta_y=\zeta_z=0.5$  m, corresponding to a heterogeneous, isotropic aquifer.

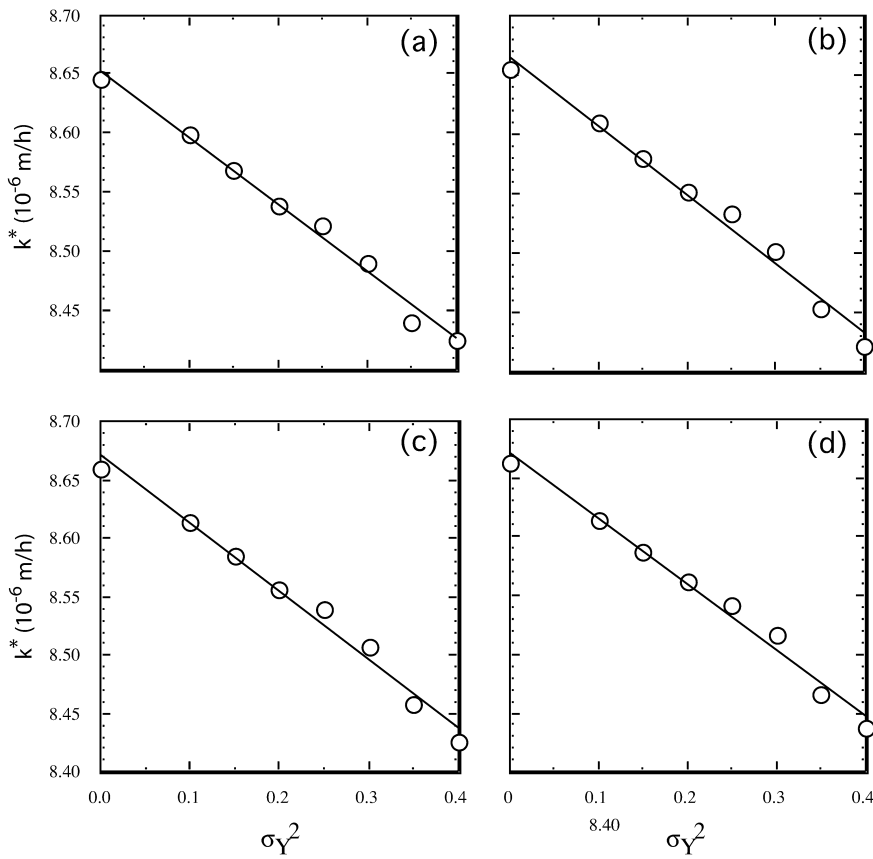


**Fig. 4**

Average mass transfer coefficient as a function of the variance of the log-transformed hydraulic conductivity distribution for  $dh/dx$  of **a** 0.0020, **b** 0.0030, **c** 0.0040, and **d** 0.0048. *Open circles* denote numerically generated data and *solid lines* denote linear fits (here,  $t=30,000$  h)

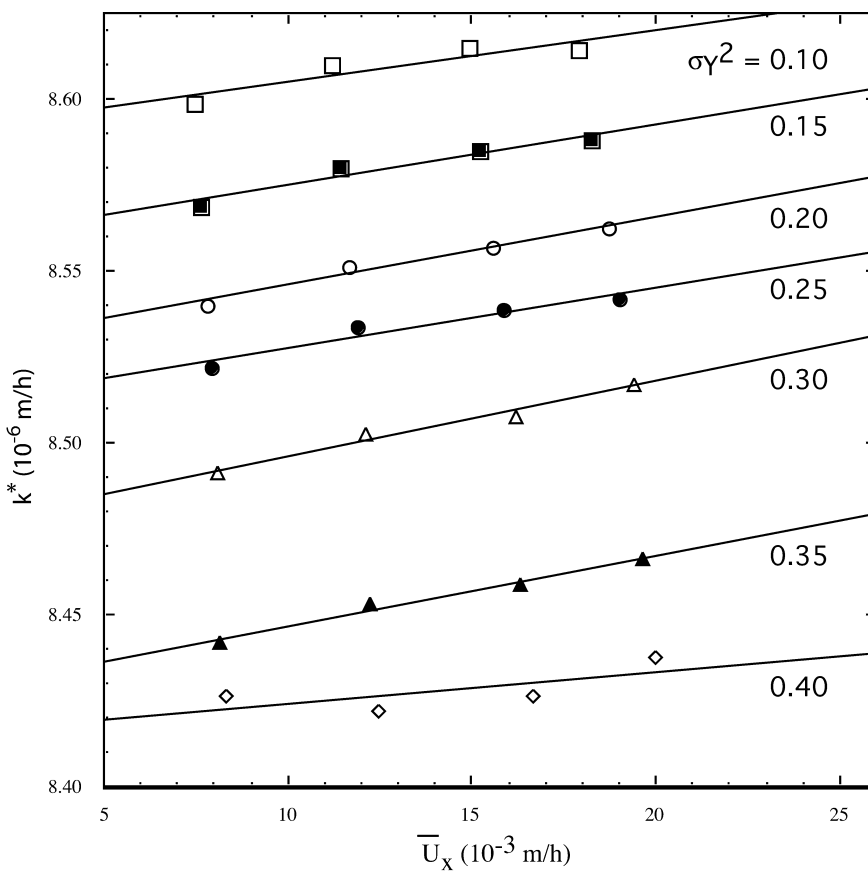


**Fig. 5**

Average mass transfer coefficient as a function of the interstitial fluid velocity along the direction of flow for various values of the variance of the log-transformed hydraulic conductivity

Groundwater interstitial velocities were varied by changing the piezometric head gradient ( $\partial h/\partial x$ ) along the longitudinal direction. The range of  $\partial h/\partial x$  examined here is from 0.0020 to 0.0048. This range in  $\partial h/\partial x$  covers regional hydraulic gradients as well as hydraulic gradients observed at pumping zones. A mean hydraulic conductivity of  $\bar{K} = 1.038$  m/h is used representing a fine to coarse sand (Bear 1979). The values of  $\sigma_Y^2$  considered in this study are: 0.00, 0.10, 0.15, 0.20, 0.25, 0.30, 0.35, and 0.40. All numerical results are evaluated at  $t=30,000$  h, representing steady-state conditions.

To evaluate the time invariant average mass transfer coefficient  $k^* = \bar{k}(t)$  as a function of the variance of the log-transformed hydraulic conductivity  $\sigma_Y^2$ , simulations were performed keeping the hydraulic gradient  $\partial h/\partial x$  constant while varying  $\sigma_Y^2$ . Figure 4 presents 32 numerically evaluated average mass transfer coefficients,  $k^*$ , for various values of  $\sigma_Y^2$  and several different hydraulic gradients. Each  $k^*$  is evaluated using Eq. (23) and represents the average of 40 different realizations of the hydraulic conductivity field for a given  $\sigma_Y^2$ . It is evident from Fig. 4 that the variance of the log-transformed hydraulic conductivity distribution is inversely proportional to the average mass transfer coefficient. A similar trend was also observed in the results of numerical experimentations of DNAPL pool dissolution in two-dimensional porous formations (Vogler and Chrysikopoulos 2001). The decrease in  $k^*$  with increasing  $\sigma_Y^2$  is attributed to the enhanced spreading of the NAPL dissolved in the aqueous phase, due to progressive increases in aquifer heterogeneity. Spreading of the aqueous phase contaminant concentration leads to a reduction in the contaminant concentration gradient above the pool-water interface. Furthermore, it should be noted that in view of Eq. (3), it is also evident that decreasing the concentration gradient normal to the DNAPL pool-water interface results in a decrease in the mass transfer coefficient.

Figure 5 illustrates the relation between  $\bar{U}_x$ ,  $\sigma_Y^2$ , and  $k^*$ . Clearly, it is evident from Fig. 5 that an increase in  $\sigma_Y^2$  leads to a decrease in  $k^*$ , and that  $k^*$  is directly proportional to  $\bar{U}_x$ . This result is in perfect agreement with theoretical (Kim and Chrysikopoulos 1999) as well as experimental (Chrysikopoulos and others 2000; Lee and Chrysikopoulos 2002) results, suggesting that by increasing the interstitial velocity or decreasing the contaminant spreading (i.e., aquifer dispersivity) leads to enhanced mass transfer from a DNAPL pool into a water-saturated porous formation.

The results presented in Figs. 4 and 5 strongly suggest that there is a correlation between  $k^*$ ,  $\sigma_Y^2$ , and  $\bar{U}_x$ . Consequently, an empirical equation describing the relationship between the mass transfer coefficient and all the appropriate parameters of the physical system can be developed.

## Mass transfer correlation

The parameters that influence greatly the time invariant average mass transfer coefficient associated with the dissolution of a single-component DNAPL pool in water-

saturated, heterogeneous aquifers are: the effective molecular diffusion coefficient,  $\mathcal{D}_e$ ; the average hydrodynamic dispersion coefficients in the longitudinal and lateral directions,  $\bar{D}_x$ , and  $\bar{D}_y$ ; the average interstitial groundwater velocities in the longitudinal and lateral directions,  $\bar{U}_x$  and  $\bar{U}_y$ ; the pool dimensions in both  $x$  and  $y$  directions,  $l_x$  and  $l_y$ ; the characteristic length of the DNAPL pool,  $l_c$ ; and the variance of the log-transformed hydraulic conductivity,  $\sigma_Y^2$ . It should be noted that the average parameters represent the arithmetic means of the local parameter values in the discrete unit elements over the entire aquifer domain.

The appropriate empirical time invariant, average mass transfer correlation relating the overall Sherwood number,  $Sh^*$ , to the variance of the log-transformed hydraulic conductivity,  $\sigma_Y^2$ ; the longitudinal direction overall Peclet number,  $Pe_x^*$ , and lateral direction overall Peclet number,  $Pe_y^*$ , can be expressed by the following power law:

$$Sh^* = 0.905(\sigma_Y^2)^{-0.017}(Pe_x^*)^{1.18}(Pe_y^*)^{0.0074}, \quad (29)$$

where

$$Sh^* = \frac{k^* l_c}{\mathcal{D}_e}, \quad (30)$$

$$Pe_x^* = \frac{\bar{U}_x l_x}{\mathcal{D}_x}, \quad (31)$$

$$Pe_y^* = \frac{\bar{U}_y l_y}{\mathcal{D}_y}, \quad (32)$$

$$l_c = (l_x l_y)^{\frac{1}{2}}. \quad (33)$$

The empirical correlation coefficients in Eq. (29) were determined by a nonlinear least squares regression of 28 numerically calculated  $Sh^*$  values for seven different  $\sigma_Y^2$  values and four hydraulic gradients ( $dh/dx=0.0020, 0.0030, 0.0040, \text{ and } 0.0048$ ), shown in Fig. 6. It should be noted that the empirical mass transfer correlation Eq. (29) is valid for  $0.1 \leq \sigma_Y^2 \leq 0.4$ .

Figure 7 presents a comparison between the Sherwood numbers computed by Eq. (30) to Sherwood numbers predicted by Eq. (29) as a function of the variance of the log-transformed hydraulic conductivity and overall Peclet number in the  $x$ -direction. A reasonable fit between the numerically computed and correlation predicted Sherwood numbers is observed.

## Summary

A numerical model for flow and transport of a contaminant originating from the dissolution of a DNAPL pool in a heterogeneous aquifer is developed. The model uses randomly generated, three-dimensional, heterogeneous, isotropic hydraulic conductivity fields with specified

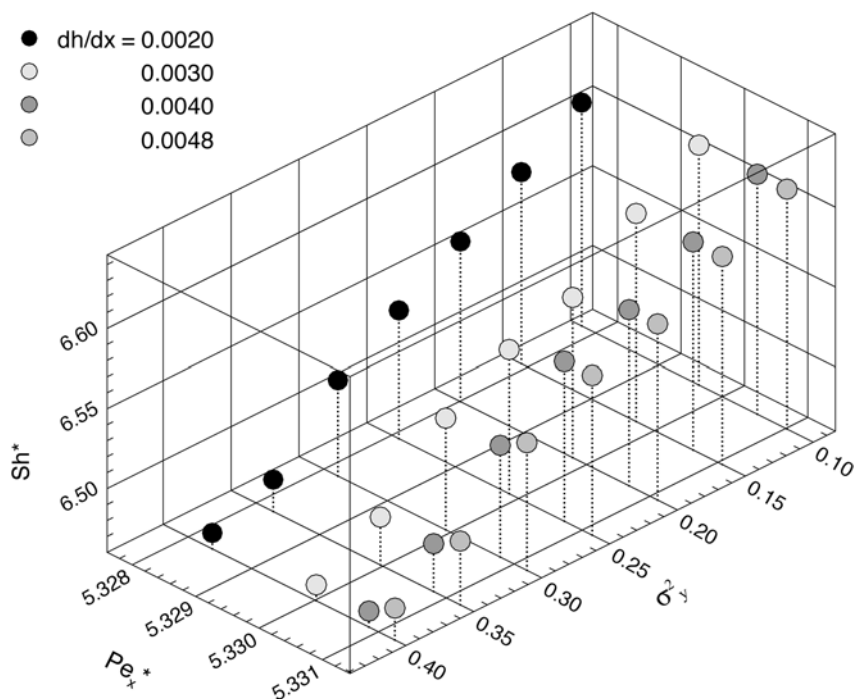


Fig. 6

Numerically determined overall Sherwood numbers as a function of  $\sigma_y^2$  and  $Pe_x^*$  for several hydraulic gradients (here,  $Pe_y^* = 0.02$ )

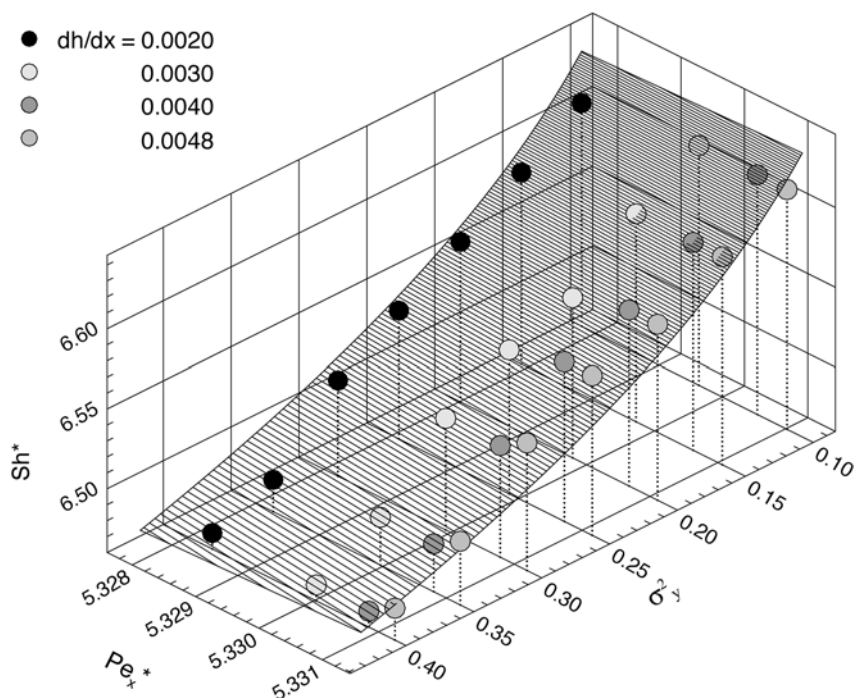


Fig. 7

Comparison of numerically determined and correlation predicted Sherwood numbers as a function of  $\sigma_y^2$  and  $Pe_x^*$  for several hydraulic gradients. Filled circles denote numerically determined data and the three-dimensional surface denotes correlation predictions (here,  $Pe_y^* = 0.02$ )

mean, variance, and correlation length scales. A linear relationship is observed between the variance of the log-transformed hydraulic conductivity and the average mass transfer coefficient. Model simulations indicate that the effect of the variance of the log-transformed hydraulic conductivity on the average mass transfer coefficient is more significant than the effect of the hydraulic gradient or equivalently the effect of the interstitial fluid velocities. A mass transfer correlation based on numerically gener-

ated data that relates the dimensionless overall mass transfer coefficient (Sherwood number) to the variance of the log-transformed hydraulic conductivity and appropriate Peclet numbers was developed. The correlation presented here can be used in existing analytical or numerical mathematical models simulating the transport of dissolved organics originating from the dissolution of NAPL pools in heterogeneous, water-saturated subsurface formations.

# Appendix

## Nomenclature

$C$	Liquid phase contaminant concentration (solute mass/liquid volume), ( $M/L^3$ )
$C_b$	Background aqueous phase contaminant concentration, ( $M/L^3$ )
$C_s$	Aqueous saturation concentration, ( $M/L^3$ )
$C_Y$	Covariance function of $Y$
$\mathcal{D}$	Molecular diffusion coefficient, ( $L^2/t$ )
$\mathcal{D}_e$	Effective molecular diffusion coefficient, equal to $\mathcal{D}/\tau^*$ , ( $L^2/t$ )
$D_x$	Longitudinal hydrodynamic dispersion coefficient, ( $L^2/t$ )
$\bar{D}_x$	Average longitudinal hydrodynamic dispersion coefficient, ( $L^2/t$ )
$D_y$	Lateral hydrodynamic dispersion coefficient, ( $L^2/t$ )
$\bar{D}_y$	Average lateral hydrodynamic dispersion coefficient, ( $L^2/t$ )
$D_z$	Vertical hydrodynamic dispersion coefficient, ( $L^2/t$ )
erf	Error function
$h$	Piezometric head, ( $L$ )
$h_0$	Upstream piezometric head, ( $L$ )
$h_L$	Downstream piezometric head, ( $L$ )
$H$	Aquifer dimension in $z$ direction, ( $L$ )
$k$	Local mass transfer coefficient, ( $L/t$ )
$\bar{k}$	Average mass transfer coefficient, ( $L/t$ )
$k^*$	Time invariant average mass transfer coefficient, ( $L/t$ )
$K$	Hydraulic conductivity, ( $L/t$ )
$\bar{K}$	Average hydraulic conductivity, ( $L/t$ )
$K_d$	Contaminant partition coefficient between the solid matrix and the aqueous phase, ( $L^3/M$ )
$l_c$	Characteristic length, ( $L$ )
$l_x$	Pool dimension in $x$ direction, ( $L$ )
$l_{x_0}$	$x$ Cartesian coordinate of the origin of a rectangular pool, ( $L$ )
$l_y$	Pool dimension in $y$ direction, ( $L$ )
$l_{y_0}$	$y$ Cartesian coordinate of the origin of a rectangular pool, ( $L$ )
$L$	Aquifer dimension in $x$ direction, ( $L$ )
$n_x, n_y, n_z$	Number of discrete unit-elements along the $x$ -, $y$ -, and $z$ -directions of the model aquifer, respectively
$N$	Total number of hydraulic conductivity field realizations
$Pe_x^*$	Overall Peclet numbers in the $x$ -direction, defined in Eq. (31)
$Pe_y^*$	Overall Peclet numbers in the $y$ -direction, defined in Eq. (32)
$\mathbf{r}$	Vector with magnitude equal to the separation distance of two $K$ measurements
$r_x$	Separation distance in the longitudinal direction of two $K$ measurements
$r_y$	Separation distance in the lateral direction of two $K$ measurements
$r_z$	Separation distance in the vertical direction of two $K$ measurements
$R$	Dimensionless retardation factor
$\mathcal{R}$	Region defined by the DNAPL-water interfacial area
$Sh^*$	Overall Sherwood number
$t$	Time, $t$
$U_x$	Interstitial fluid velocity in the longitudinal direction, ( $L/t$ )
$\bar{U}_x$	Average interstitial fluid velocity in the longitudinal direction, ( $L/t$ )
$U_y$	Interstitial fluid velocity in the lateral direction, ( $L/t$ )
$\bar{U}_y$	Average interstitial fluid velocity in the lateral direction, ( $L/t$ )
$U_z$	Interstitial fluid velocity in the vertical direction, ( $L/t$ )
$W$	Aquifer dimension in $y$ direction, ( $L$ )
$x$	Longitudinal spatial coordinate, ( $L$ )

$y$	Lateral spatial coordinate, ( $L$ )
$Y$	Log-transformed hydraulic conductivity, equal to $\ln K$
$z$	Vertical spatial coordinate, ( $L$ )

## Greek letters

$\alpha_L$	Longitudinal dispersivity, ( $L$ )
$\alpha_T$	Transverse dispersivity, ( $L$ )
$\zeta_x$	Correlation length in the longitudinal direction, ( $L$ )
$\zeta_y$	Correlation length in the lateral direction, ( $L$ )
$\zeta_z$	Correlation length in the vertical direction, ( $L$ )
$\theta$	Porosity (liquid volume/aquifer volume), ( $L^3/L^3$ )
$\kappa_1, \kappa_2$	Defined in Eqs. (25) and (26), respectively
$\xi_1, \xi_2$	Defined in Eqs. (27) and (28), respectively
$\rho_b$	Bulk density of the solid matrix, ( $M/L^3$ )
$\sigma_Y^2$	Variance of $\ln K$
$\tau$	Dummy integration variable
$\tau^*$	Tortuosity coefficient ( $\geq 1$ )

## Abbreviations

ADI	Alternating direction implicit
DNAPL	Dense nonaqueous phase liquid
NAPL	Nonaqueous phase liquid
1,1,2-TCA	1,1,2-Trichloroethane

## References

- Anderson MR, Johnson RL, Pankow JF (1992) Dissolution of dense chlorinated solvents into groundwater, 3, Modeling contaminant plumes from fingers and pools of solvent. *Environ Sci Technol* 26(5):901–908
- Bear J (1979) *Hydraulics of groundwater*. McGraw-Hill, New York
- Christakos G (1992) *Random field models in earth sciences*. Academic Press, San Diego
- Chrysikopoulos CV (1995a) Three-dimensional analytical models of contaminant transport from nonaqueous phase liquid pool dissolution in saturated subsurface formations. *Water Resour Res* 31:1137–1145
- Chrysikopoulos CV (1995b) Effective parameters for flow in saturated heterogeneous porous media. *J Hydrol* 170:181–197
- Chrysikopoulos CV, Lee KY (1998) Contaminant transport resulting from multicomponent phase liquid pool dissolution in three-dimensional subsurface formations. *J Contam Hydrol* 31(1–2):1–21
- Chrysikopoulos CV, Kim T-J (2000) Local mass transfer correlations for nonaqueous phase liquid pool dissolution in saturated porous media. *Trans Porous Media* 38(1–2):167–187
- Chrysikopoulos CV, Voudrias EA, Fyrrillas MM (1994) Modeling of contaminant transport resulting from dissolution of nonaqueous phase liquid pools in saturated porous media. *Trans Porous Media* 16(2):125–145
- Chrysikopoulos CV, Lee KY, Harmon TC (2000) Dissolution of a well-defined trichloroethylene pool in saturated porous media: experimental design and aquifer characterization. *Water Resour Res* 36(7):1687–1696
- Chrysikopoulos CV, Hsuan P-Y, Fyrrillas MM (2002) Bootstrap estimation of the mass transfer coefficient of a dissolving nonaqueous phase liquid pool in porous media. *Water Resour Res* 38(3):10.1029/2001WR000661

- Dagan G (1989) Flow and transport in porous formations. Springer, Berlin Heidelberg New York
- Dela Barre BK, Harmon TC, Chrysikopoulos CV (2002) Measuring and modeling the dissolution of nonideally shaped dense nonaqueous phase liquid (NAPL) pools in saturated porous media. *Water Resour Res* 38(8):10.1029/2001WR000444
- Freeze RA (1975) A stochastic-conceptual analysis of one-dimensional groundwater flow in nonuniform homogeneous media. *Water Resour Res* 11(5):725–741
- Gelhar LW, Axness CL (1983) Three-dimensional stochastic analysis of macrodispersion in aquifers. *Water Resour Res* 19(1):161–180
- Gutjahr AL (1999) SF3D, random field generator. New Mexico Institute of Mining and Technology, Socorro, New Mexico
- Holman H-YN, Javandel I (1996) Evaluation of transient dissolution of slightly water soluble compounds from a light nonaqueous phase liquid pool. *Water Resour Res* 32(4):915–923
- Johnson RL, Pankow JF (1992) Dissolution of dense chlorinated solvent into groundwater. 2. Source functions for pools of solvent. *Environ Sci Technol* 26(5):896–901
- Kim T-J, Chrysikopoulos CV (1999) Mass transfer correlations for nonaqueous phase liquid pool dissolution in saturated porous media. *Water Resour Res* 35(2):449–459
- Khachikian C, Harmon TC (2000) Nonaqueous phase liquid dissolution in porous media: current state of knowledge and research needs. *Trans Porous Media* 38(1–2):3–28
- Lee KY, Chrysikopoulos CV (1995) Numerical modeling of three-dimensional contaminant migration from dissolution of multi-component NAPL pools in saturated porous media. *Environ Geol* 26(3):157–165
- Lee KY, Chrysikopoulos CV (1998) NAPL pool dissolution in stratified and an-isotropic porous formations. *J Environ Eng*:851–860
- Lee KY, Chrysikopoulos CV (2002) Dissolution of a well-defined trichloroethylene pool in saturated porous media: experimental results and model simulations. *Water Res* 36:3911–3918
- Leij FJ, van Genuchten MTh (2000) Analytical modeling of nonaqueous phase liquid dissolution with Green's functions. *Trans Porous Media* 38(1–2):141–166
- Mackay D, Shiu WY, Ma KC (1992) Illustrated handbook of physical-chemical properties and environmental fate for organic chemicals. 3. Volatile organic chemicals. Lewis, Chelsea, MI
- Mason AR, Kueper BH (1996) Numerical simulation of surfactant-enhanced solubilization of pooled DNAPL. *Environ Sci Technol* 30:3205–3215
- Press WH, Flannery BP, Teukolsky SA, Vetterling WT (1992) Numerical recipes: the art of scientific computing, 2nd edn. Cambridge University Press, New York
- Rivett MO, Feenstra S, Cherry JA (1994) Transport of a dissolved phase plume from a residual solvent source in a sand aquifer. *J Hydrol* 159(1–4):27–41
- Russo D, Zaidel J, Laufer A (1994) Stochastic analysis of solute transport in partially saturated heterogeneous soils. 1. Numerical experiments. *Water Resour Res* 30(3):769–779
- Sciortino A, Harmon TC, Yeh W-G (2000) Inverse modeling for locating dense nonaqueous pools in groundwater under steady flow conditions. *Water Resour Res* 36(7):1723–1735
- Seagren EA, Rittmann BE, Valocchi AJ (1999) An experimental investigation of NAPL pool dissolution enhancement by flushing. *J Contam Hydrol* 37:111–137
- Sudicky EA (1986) A natural gradient experiment on solute transport in a sand aquifer: Spatial variability of hydraulic conductivity and its role in the dispersion process. *Water Resour Res* 22(13):2069–2082
- Tatalovich ME, Lee KY, Chrysikopoulos CV (2000) Modeling the transport of contaminants originating from the dissolution of DNAPL pools in aquifers in the presence of dissolved humic substances. *Trans Porous Media* 38(1–2):93–115
- Vogler ET, Chrysikopoulos CV (2001) Dissolution of nonaqueous phase liquid pools in anisotropic aquifers. *Stochastic Environ Res Risk Assess* 15:33–46